Electro-organic Synthesis of some Cyclopentanone Derivatives

Magdi A. Azzem
El Monoufia University, El Monoufia, Cairo, Egypt
Gald E. H. Elgemeie
Bani Suef Branch, Cairo University, Cairo, Egypt
Mohamed A. Neguid and Hussein M. Fahmy*
Department of Chemistry, Faculty of Science, Cairo University, Giza, Egypt
Zakeya M. Elmassry
Department of Science, The American University in Cairo, Egypt

The electroreduction of some benzothiazole derivatives in aqueous media has been studied. A mechanism is suggested and discussed for the formation of the cyclopentanone derivatives which were isolated and identified. The mechanism proposed has been confirmed by polarographic analyses, cyclic voltammetry, spectrophotometric pK_a determination, identification of CPE products, and the study of Hammett relations.

Recently workers in our laboratory have investigated the electroreduction of a series of thiadiazole derivatives[1,2] substituted by an activated alkenic bond in which a Ziegler–Thorp reaction[3] took place and cyclopentene derivatives were obtained. It therefore seemed of value to study the electroreduction of some related benzothiazole derivatives in order to test the effect of the hetero-activated ring on the feasibility of the Zeigler–Thorp reaction. In the present investigation a series of 1,3-benzothiazol-2-yl (4-substituted) cinnamonitrile derivatives (**1a–d**) together with a model compound, namely 2-cyanomethyl-1,3-benzothiazole (**2**), in alcoholic buffered media, have been examined in order to shed light on the electrochemistry of the benzothiazole ring which has proved to have pronounced medical and pharmaceutical activities.[4–6]

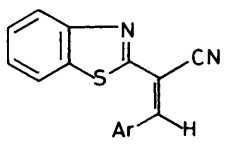

Ar

(**1a**) Ph
(**1b**) 4-ClC_6H_4
(**1c**) 4-$MeOC_6H_4$
(**1d**) 4-$NO_2C_6H_4$

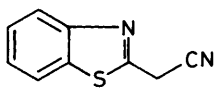

(**2**)

Experimental

(*d*) *Organic Synthesis.*—A suspension of 2-cyanomethyl-1,3-benzothiazole[6] (0.01 mol) in ethanol (10 cm^3) and triethylamine was treated with aromatic aldehyde (0.01 mol). The reaction mixture was refluxed for 2 h then evaporated under reduced pressure. The remaining solid product was collected by filtration and recrystallised from the appropriate solvent (see Table 1).

Polarography.—(i) *Apparatus. i–E* curves were recorded with a Wenking potentioscan (POS 73) in conjunction with *x–y* recorder (PL3) JJ-instruments. The capillary characteristics in H_2O open circuit are: t = 2.7 s per drop and m = 1.3 mg s^{-1} for h = 55 cm. A conventional three-electrode system was used with an SCE as the reference. The $E_{\frac{1}{2}}$ values were measured graphically with an accuracy of ±0.005 V. The pH measurements were performed with a digital pH-meter (Ministis 5000, Tacussel).

(ii) *Solutions.* Stock solutions (10^{-3} mol dm^{-3}) were prepared by dissolving an accurately weighed quantity of material in the appropriate volume of absolute ethanol. Britton–Robinson buffers[7] were used as the supporting electrolyte.

(iii) *Procedure.* Ethanol (3 cm^3) and buffer solution (5 cm^3) were introduced into the cell. The mixture was de-areated with hydrogen for 10 min. Reactant (2 cm^3; 10^{-3} mol dm^{-3}) was introduced in the cell such that the final concentration was 2×10^{-4} mol dm^{-3} in 10 cm^3 of 50% (v/v) ethanolic buffer.

(*c*) *Controlled Potential Electrolysis* (CPE) *and Identification of the Resulting Products.*—Electrolysis was performed on the two compounds (**1a,c**), which are taken to be representative examples for the series studied.

(i) Electrolysis of (**1a**) (150 mg), in ethanol–conc. HCl (60:40) was carried out. The electrolysis cell was a 250 cm^3 flask, into which gas inlet, reference and auxiliary electrodes were introduced. The potential was fixed at −1.0 V *vs.* SCE. The progress of electrolysis was followed by recording the decay in current with time; this began with a value of 50 mA and dropped over an interval of 3 h to 4 mA. The resulting turbid solution was partially evaporated to a tenth of its original volume. The precipitated product was filtered off and recrystallised from ethanol. The pale yellow product obtained (*ca.* 70%) had the following characteristics: m.p. 88 °C; ν_{max}(KBr) 2 220 (CN), and 1 720 cm^{-1} (CO); *m/z* 527, 391, 346, 265, 212, 136, 126, 105, and 91; δ_H([$^2H_6$]DMSO) 3.3–3.45 (m, 3 H, 3CH) and 6.8–7.8 (m, 18 H, 2Ph + $2C_6H_4$) and was identified as 2,5-bis(1,3-benzothiazol-2-yl)-2-cyano-3,4-diphenylcylopentanone.

(ii) The previous procedure was performed following the electrolysis of 260 mg of compound (**1c**) in ethanol–conc. HCl (70:30) at −1.0 V *vs.* SCE. The current was initially 70 mA and dropped within 4 h to 3 mA. The orange product resulting from electrolysis had the following characteristics: m.p. 110 °C; ν_{max} 1 720 (CO) and 2 220 cm^{-1} (CN); δ_H([$^2H_6$]DMSO) 3.68–3.80 (m, 3 H, 3CH), 3.84 (s, 3 H, OMe), 3.88 (s, 3 H, OMe), and 6.85–8.4 (m, 16 H, $4C_6H_4$) (Found: C, 70.0; H, 4.3; N, 7.6. $C_{34}H_{25}N_3O_3S_2$ requires C, 69.5; H, 4.3; N, 7.2; S, 10.9%). This product was identified as 2,5-bis(1,3-benzothiazol-2-yl)-2-cyano-3,4-bis(4-methoxyphenyl)cyclopentan-1-one.

Table 1. Characteristic data for compounds (**1a–d**).

Compound	Colour	Yield (%)	M.p./°C	Formula	*M*	ν/cm^{-1}	δ_H (ppm)
(**1a**)	Yellow	80	122–123	$C_{16}H_{10}N_2S$	262.3	2 220 (CN)	7.2–7.6 (m, 5 H, Ph); 7.7–8.1 (m, 4 H, C_6H_4); 8.3 (s, 1 H, ylidenic CH).
(**1b**)	Yellow	70	149–150	$C_{16}H_9ClN_2S$	296.8	2 225 (CN)	7.1–7.8 (m, 4 H, C_6H_4); 7.9–8.2 (m, 4 H, C_6H_4); 8.3 (s, 1 H, ylidenic CH).
(**1c**)	Orange	75	144–145	$C_{17}H_{12}N_2OS$	292.2	2 220 (CN)	3.95 (s, 3 H, OMe); 7.1–7.65 (m, 4 H, C_6H_4); 7.80–8.3 (m, 4 H, C_6H_4); 8.2 (s, 1 H, ylidenic CH).
(**1d**)	Yellow	70	148–149	$C_{16}H_9N_3O_2S$	307.3	2 220 (CN)	7.12–7.62 (m, 4 H, C_6H_4); 7.70–8.20 (m, 4 H, C_6H_4); 8.26 (s, 1 H, ylidenic CH).

Table 2. pK_a values for compounds (**1a–d**) and model compound (**2**).

Compound	pK_a (1)	pK_a (2)
(**1a**)	2.8	9.2
(**1b**)	2.6	9.0
(**1c**)	2.9	10.4
(**1d**)	2.3	8.0
(**2**)	2.8	10.1

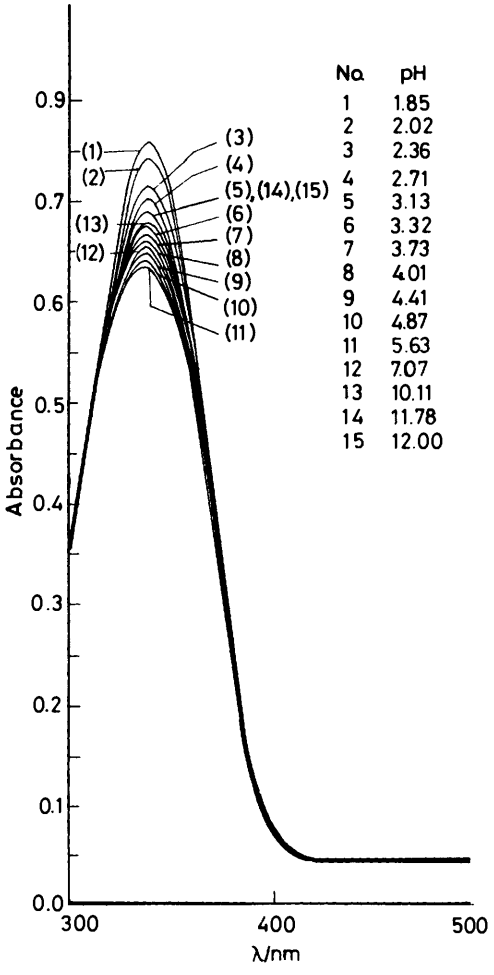

Figure 1. Electronic absorption spectra of (**1a**) (3 × 10^{-5} mol dm^{-3}) in ethanol–water (50%, v/v).

(*d*) *Spectrophotometry and Determination of* pK_a *Values.*—The absorption spectra of (**1a–d**) and (**2**) were scanned on a Perkin-Elmer λ_3 spectrophotometer over the wavelength range

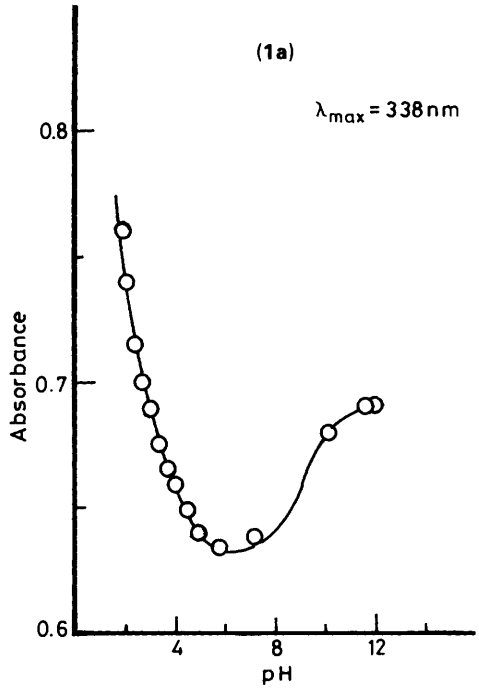

Figure 2. Absorbance *vs.* pH plot of (**1a**) (3 × 10^{-5} mol dm^{-3}) in ethanol–water (50%, v/v).

200–500 nm. For this purpose a solution of compound (3 cm^3, 10^{-3} mol dm^{-3}) was mixed with $HClO_4$ (5 cm^3, 1 mol dm^{-3}; 50% v/v ethanolic water mixture). The variation in pH values was achieved by adding each time a very small amount of conc. NaOH (carbonate free). The absorption spectra of (**1a**) showed a strong band with λ_{max} 338 nm. The variation of spectra with increasing pH is illustrated in Figure 1. The corresponding absorbance pH curve is illustrated in Figure 2. All curves for (**1a–d**) and (**2**) showed two pK_a values corresponding to a sharp increase or decrease in absorbance, and these values are displayed in Table 2.

Results and Discussion

(*a*) *Polarographic Behaviour.*—The polarograms of (**1a**) (2 × 10^{-4} mol dm^{-3}), taken as a representative example, are illustrated in Figure 3. At pH <6.8 one well-defined cathodic wave A_1 with limiting current $i_l(a_1)$, which corresponds to a one-electron transfer, is displayed. At higher pH values another wave A_2 appears which is equal in height to A_1. As the pH of solution increases further the limiting currents of both waves A_1 and A_2 decrease in the form of dissociation curves. At pH >8.9 a third wave B appears and its i_l value simultaneously increases in value with increase of pH. Typical plots of $E_{\frac{1}{2}}$ and i_l *vs.* pH for these waves are illustrated graphically in Figure 4 for (**1a**). Shifts

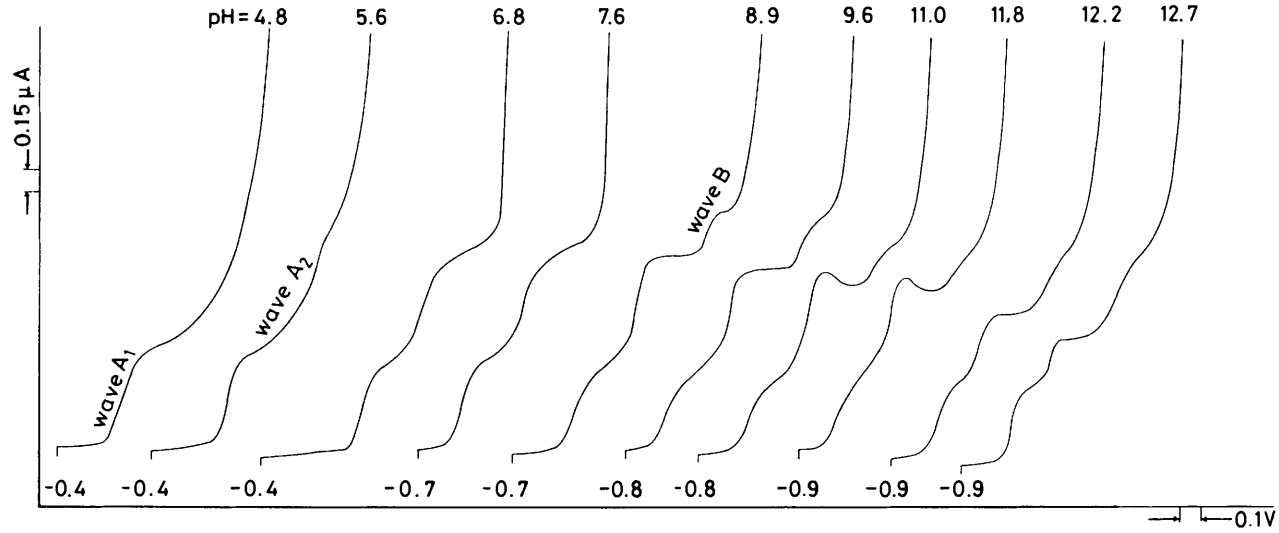

Figure 3. Schematic representation of the polarograms of (**1a**) in ethanolic Britton–Robinson buffers (50%, v/v).

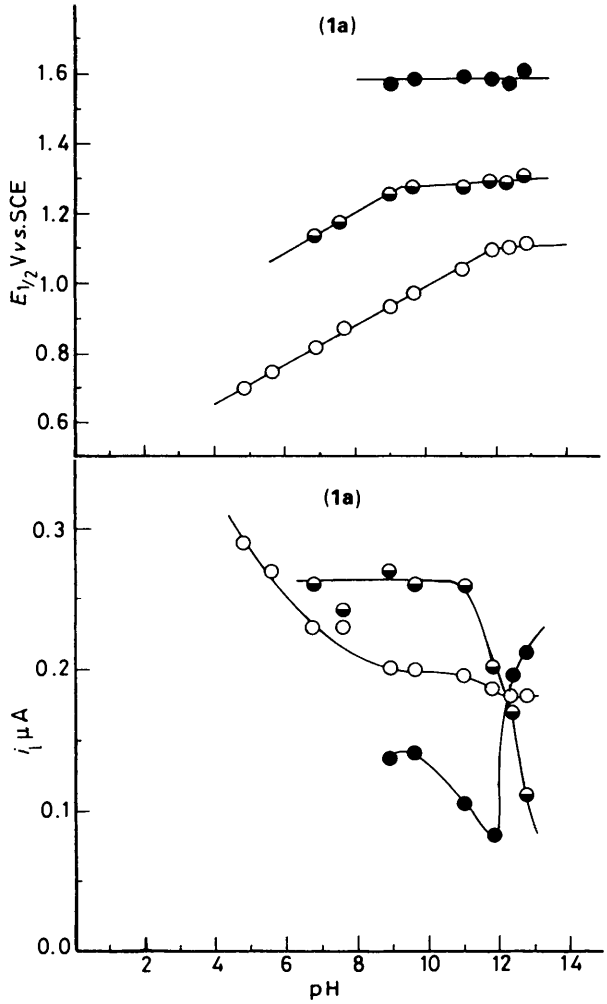

Figure 4. $E_{\frac{1}{2}}$, i_l *vs.* pH plot of the polarographic waves of (**1a**) (1×10^{-4} mol dm^{-3}) in ethanolic Britton–Robinson buffers (50%, v/v). ○, wave A_1; ◒, wave A_2; ●, wave B.

of $E_{\frac{1}{2}}$ with increase in pH for all compounds are compiled in the form of linear equations in Table 3. It is clear for (**1a**) (Figure 4) that the $E_{\frac{1}{2}}$–pH plots of waves A_1 and A_2 show mainly two

Table 3. Linear representation of $E_{\frac{1}{2}}$–pH dependence for waves A_1 and A_2 of compounds (**1a–d**).

	$E_{\frac{1}{2}}$–pH equations[a]	
Compound	Wave A_1	Wave A_2
(**1a**)	$E_{\frac{1}{2}} = -0.43 - 0.056$ pH	$E_{\frac{1}{2}} = -0.74 - 0.057$ pH
(**1b**)	$E_{\frac{1}{2}} = -0.35 - 0.063$ pH	$E_{\frac{1}{2}} = -0.67 - 0.062$ pH
(**1c**)	$E_{\frac{1}{2}} = -0.55 - 0.056$ pH	$E_{\frac{1}{2}} = -0.91 - 0.043$ pH
(**1d**)	$E_{\frac{1}{2}} = -0.52 - 0.068$ pH	$E_{\frac{1}{2}} = -0.61 - 0.065$ pH
	$E_{\frac{1}{2}} = +0.045 - 0.054$ pH ... (C)	
	$E_{\frac{1}{2}} = -0.58 - 0.038$ pH ... (D)	

[a] Equations C and D are those corresponding to the reduction of the NO_2 group.

segments, in one of which $E_{\frac{1}{2}}$ is pH sensitive, while in the other $E_{\frac{1}{2}}$ is independent of pH. On the other hand the half-wave potential of wave B is practically independent of variation with pH. The intersection of the two segments of wave A_1 gives a value which is approximately equal to the apparent dissociation constant, pK', which is in turn equal to the value of the intersection point between waves A_1, A_2 and B. On the other hand, the intersection of the two segments of wave A_2 gives values compatible with the pK_a(2) values obtained spectrophotometrically (see Table 2). In addition to waves A_1, A_2 and B, compound (**1d**) (nitro derivative) showed two additional four-and two-electron irreversible waves corresponding to the reduction of the nitro group (waves C and D) in the well-known classical reduction steps.[8] A direct comparison of the limiting currents $i_l(a_1)$, and $i_l(a_2)$ and their sum with the limiting currents of the nitro waves indicates that one electron is transferred in each of waves A_1 and A_2. This was also confirmed by calculating the number of electrons with an electronic integrator. Logarithmic analysis of the waves at different pH values using the fundamental polarographic wave equation indicated that the electrode processes A_1 and A_2 are reversible in nature at pH <7.6, whereas at pH >8 the processes are irreversible as revealed from their calculated αn values (see Table 4). Cyclic voltammetry in a highly acidic medium (HCl, 4.7 mol dm^{-3}) shows that at high scan rates the peak at the anodic direction increases in height. The ratio $i_{p(a)}/i_{p(c)}$ as a function of scanning rate is given in Figure 5. This may indicate that the process is an EC mechanism,[9] which is irreversible in nature at low scan rates while, at high scan rates, the process is reversible.

Table 4. Data for the logarithmic analysis of waves A_1, A_2 and B for compounds (**1a–d**) (2×10^{-4} mol dm^{-3}) in ethanolic Britton–Robinson buffers (50%, v/v).

		Wave A_1		Wave A_2		Wave B	
Compound	pH[a]	$RT/\alpha nF$[b]	αn[c]	$RT/\alpha nF$	αn	$RT/\alpha nF$	αn
(**1a**)	4.8	0.055	1.072				
	7.6	0.047	1.240	0.054	1.094		
	12.7	0.031	1.894	0.031	1.890	0.061	0.962
(**1b**)	4.8	0.040	1.477				
	7.6	0.026	2.247	0.070	0.804		
	12.7	0.033	1.770	0.030	1.970	0.065	0.899
(**1c**)	4.8	0.047	1.241				
	7.6	0.013	4.282	0.059	0.998		
	12.7	0.018	3.126	0.046	1.262	0.052	1.121
(**1d**)	4.4	0.027	2.149	0.044	1.325		
	6.8	0.027	2.180	0.058	1.017		
	10.5	0.057	1.026	0.057	1.027	0.037	1.584

[a] Individual pH values at which logarithmic analysis was carried out. [b] Slopes of the straight lines obtained. [c] Transfer coefficients.

Table 5. Results of the statistical treatment of $E_{\frac{1}{2}}$–σ data for compounds (**1a–d**).

		σ			σ°			σ⁺		
pH	Wave	r[a]	ρ[b]	s.d.[c]	r	ρ	s.d.	r	ρ	s.d.
4.8	A_1	0.9908	0.2181	0.0113	0.9757	0.3044	0.0184	0.9840	0.1239	0.0149
11.8		0.9782	0.2243	0.0181	0.9538	0.3099	0.0263	0.9892	0.1298	0.0128
11.8	A_2	0.9984	0.2156	0.0045	0.9752	0.2985	0.0182	0.9807	0.1212	0.0161
11.8	B	0.9784	0.1327	0.0107	0.9350	0.1797	0.0183	0.9999	0.0776	0.0148

[a] Correlation coefficient. [b] Slope. [c] Standard deviation.

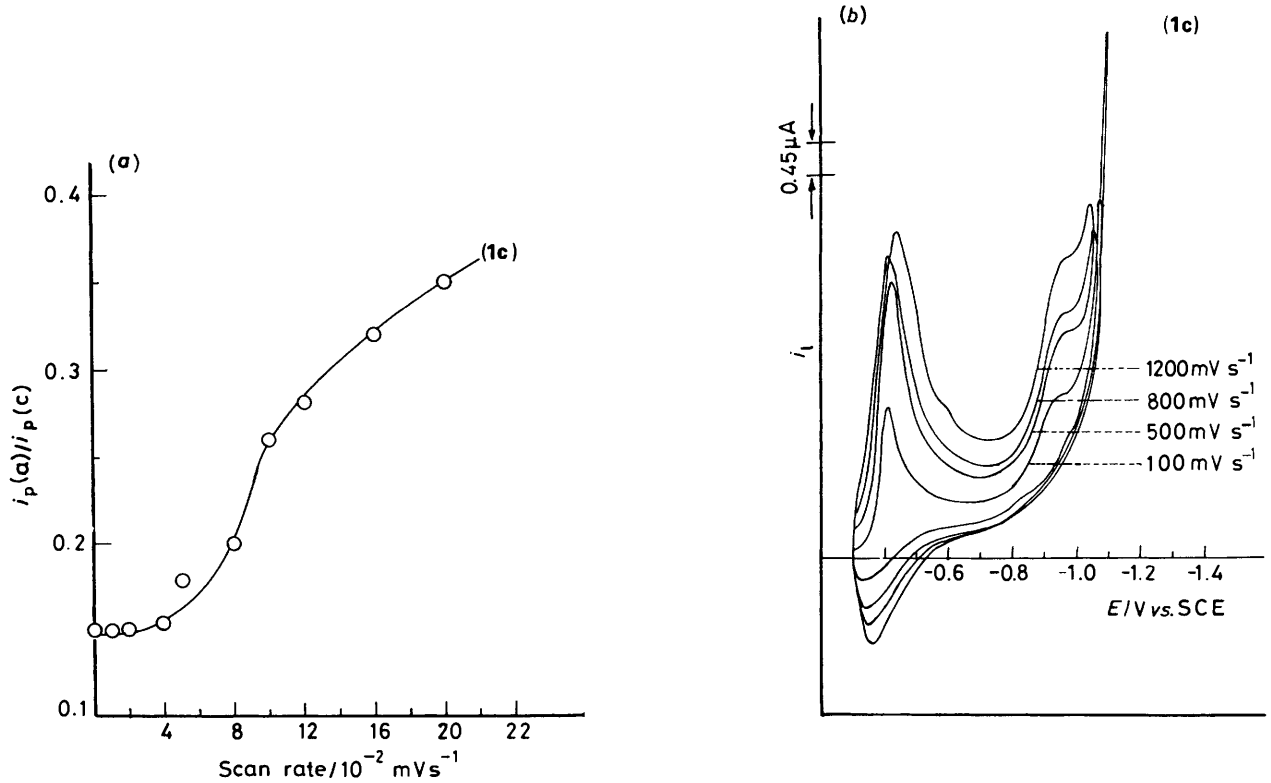

Figure 5. (*a*) Plot of the ratio of anodic to cathodic peak currents [$i_p(a)/i_p(c)$] as a function of scan rate. ○, wave A_1. (*b*) Typical cyclic voltammograms for compound (**1c**), scales and scan rates are given on the plot. [HCl] = 4.7 mol dm^{-3}.

(*b*) *Spectrophotometry.*—The spectra of (**1a**) taken as representative examples, are illustrated in Figure 1. In acid these spectra were characterised by a sharp band with λ_{max} 338 nm. A further increase in pH is associated with a relative decrease in absorbance of this band. At pH values >7 no remarkable change in absorbance with variation in pH is observed. In alkaline media the spectra showed an increase in absorbance up to pH 11.5. Immediately after this the band vanished and a new band formed at lower wavelength (blue shift). From the preceding results it may be concluded that the change in spectra is due to the shift in two equilibria as demonstrated in Scheme 1.

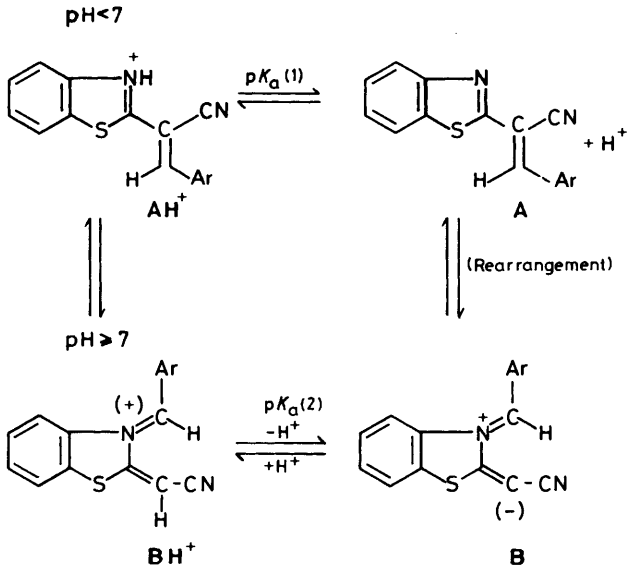

Scheme 1.

The rearrangement at pH >7 is suggested by the similarity to the 2-benzimidazol-2-yl (4-substituted) cinnamonitriles which have been synthesized and studied in some detail by one of us.[10] The idea of hydrolysis of the benzothiazole ring can be discounted since the UV spectrum shows no substantial variation in its general features in alkaline media. Finally, the concept of a diprotonated species can be discounted since $dE_{\frac{1}{2}}/d[pH]$ shifts indicate a monoprotonation process. One possibility remains for the explanation of $pK_a(2)$; this is the release of the vinylic proton from the isomeric structure BH^+. Based on the foregoing results, Scheme 2 is suggested as the explanation of the mechanism for electrode process occurring in acid media. The reaction which takes place in step (3), between a molecule of the starting material and the free radical obtained from a one-electron uptake in step (2), is confirmed by cyclic voltammetry which indicates a predominant EC mechanism. The preprotonation of the molecule is justified by the fact that wave A_1 is pH-dependent and the slope of the $E_{\frac{1}{2}}$ *vs.* pH plot is equal to *ca.* 0.06, which is an indication that a proton is involved in the preprotonation of the molecule.[11] Also, at high scanning rates the free radical is evident since the chemical reaction is comparatively slow compared with these high rates. On the other hand, $i_p(a)$ vanishes at slow scan rates since the free radical has sufficient time to react according to step (2) to give a radical dimer [step (3)]. Wave A_2 is apparently due to an EC mechanism which in the normal polarographic and CPE scales is considered to be irreversible, since acid hydrolysis and cyclisation of the product seems to be a highly compatible subsequent reaction [step (4)]. This can be anticipated since the CPE of both compounds (**1a**) and (**1c**) in conc. HCl (40%) gave the cyclised products in good yields (see the Experimental). In alkaline media the predominant form is most probably BH^+

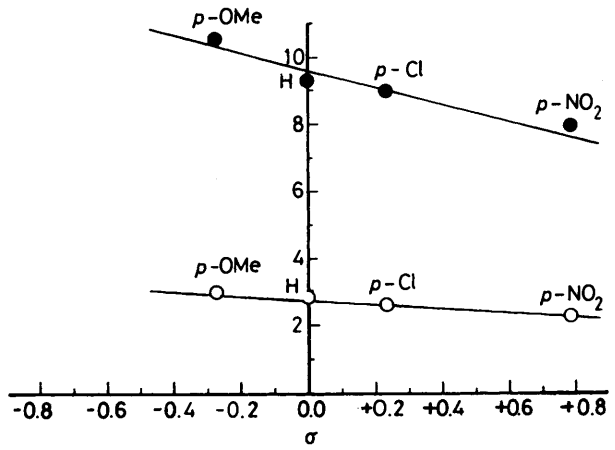

Figure 6. σ *vs.* pK_a plots for (**1a–d**). △, $pK_a(1)$; ●, $pK_a(2)$.

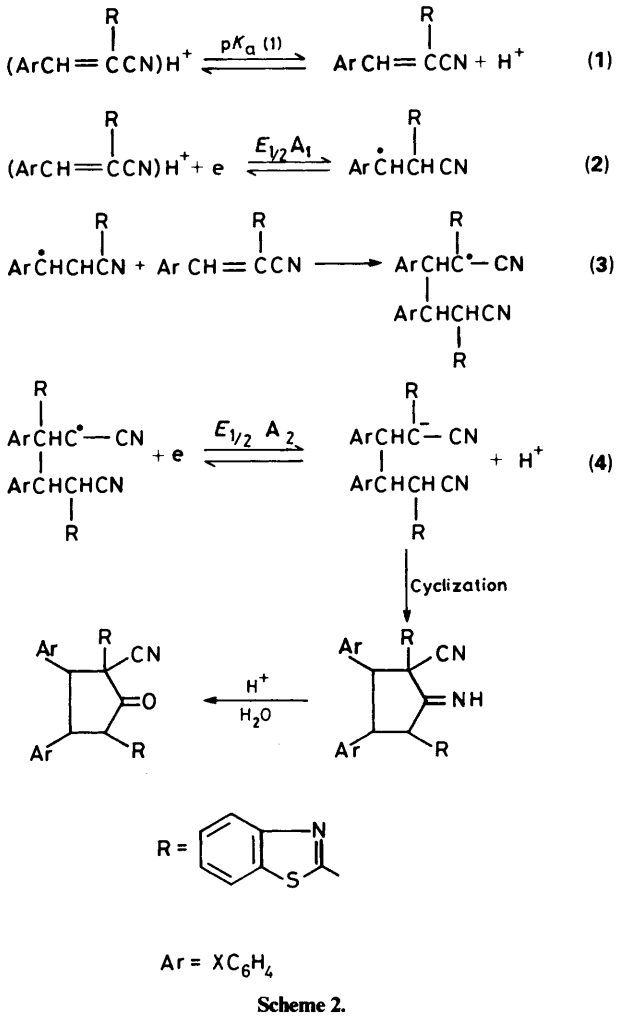

Scheme 2.

which loses H^+ to give **B** which can simultaneously rearrange to give **A** (Scheme 1). This form could possibly be further reduced. For further confirmation of the validity of both Schemes 1 and 2, it was found of interest to study both pK_a–σ and $E_{\frac{1}{2}}$–σ relations in order to elucidate individual steps in both Schemes. As is obvious from the statistical correlation of the data using Jafé calculations,[2] $pK_a(1)$ is almost unaffected by varying substitution on the benzene ring, which confirms the fact that $pK_a(1)$ is due to protonation of the molecule and not to the

ionization of a hydrogen atom included in the structure, while $pK_a(2)$–σ relation indicates that the second ionization is fairly dependent on the substituents [Figure (6)]. This is to be expected since a state of conjugation exists between the substituent and the ionizable centre as illustrated by steps $BH^+ \rightleftharpoons B + H^+$ in Scheme 1. On the other hand, it is clear that substituents affect the reduction centre; thus molecules with electron-donating groups are reduced at more negative potentials than those with electron-withdrawing substituents. The ρ values indicate that $E_{\frac{1}{2}}$ data are better correlated with σ and σ° rather than σ^+. This finding suggests that the conjugation of the substituent with the electroactive centre (C=C) is not important enough to produce a pronounced effect (Table 5).

References

1 H. M. Fahmy, N. F. Abdel Fattah, M. R. H. Elmoghayar, and M. Abdel Azzem, *J. Chem. Soc., Perkin Trans. 2*, 1988, 1.
2 M. Abdel Azzem, M. M. M. Ramiz, E. A. Ghali, H. M. Fahmy, and M. R. H. Elmoghayar, *Monatsh. Chem.*, 1987, **118**, 229.
3 S. Wawzonek, A. R. Zigman, and G. R. Hansen, *J. Electrochem. Soc.*, 1970, **117**, 1351.
4 N. M. Fathy and G. E. H. Elgemeie, *Sulphur Lett.*, 1988, **7**, 189.
5 G. E. H. Elgemeie, N. M. Fathy, and F. M. Abdel Motti, *Archiv. Pharm. (Weinheim, Ger.)*, 1988, **321**, 509.
6 G. E. H. Elgemeie and F. A. M. Abd Elaal, *Heterocycles*, 1986, **24**, 349.
7 H. T. S. Britton, 'Hydrogen Ions,' 4th edn., vol. 1, Chapman and Hall, London, 1955, p. 365.
8 H. Lund, 'Cathodic Reduction of Nitro Compounds in Organic Electrochemistry,' ed. M. M. Baizer, Dekker, New York, 1973, ch. VII, p. 315.
9 R. S. Nicholson and I. Shain, *Anal. Chem.*, 1964, **36**, 106.
10 M. A. Hammad, G. A. Nawar, and G. H. Elgemeie, *Heterocycles*, 1985, **23**, 2117.
11 S. G. Mairanovskii, *J. Electroanal. Chem. Interfacial Electrochem.*, 1962, **4**, 166.

Paper 9/00413K
Received 25*th January* 1989
Accepted 13*th November* 1989